

An Improved Method for Obtaining the Water Content Values of Ice Hydrometeors from Aircraft and Radar Data

VERNON G. PLANK, ROBERT O. BERTHEL AND ARNOLD A. BARNES, JR.

Air Force Geophysics Laboratory, Bedford, MA 01731

(Manuscript received 5 February 1980 in final form 22 August 1980)

ABSTRACT

Uncertainty analyses and operational experience at the Air Force Geophysics Laboratory (AFGL) have shown that for single samples of ice hydrometeors, the factor $\kappa = M/\sqrt{Z}$, where M (spectral liquid water content) and Z (spectral radar reflectivity factor) are computed from aircraft particle size information, is less subject to the uncertainties of converting the physical size of the particles into equivalent melted diameter than are M and Z themselves. Consequently, in correlating multiple-sample aircraft data with simultaneously acquired, independent radar measurements of Z_R , there is an appreciable accuracy enhancement that can be attained in the derivation of M vs Z equations by regression means, if κ is used as the correlation parameter, versus Z_R , rather than if spectral M is used as the correlation parameter.

1. Introduction

During the last seven years, the Air Force Geophysics Laboratory (AFGL) has provided values of the liquid water content of storm hydrometeors along the trajectories of aerospace vehicles which were deliberately flown through storms.^{1,2} Carefully calibrated, high-power radars were used to obtain the real-time Z_R values along the trajectories. Pre-launch and post-launch correlation flights were also made using instrumented aircraft that were tracked by radars at various sampling altitudes within the storms. The radar Z_R values of the hydrometeors along the aircraft flight paths were obtained in a manner such as to exclude the returns from the aircraft. Particle Measuring Systems, PMS (Knollenberg, 1970) and other instruments aboard the aircraft were used to determine the particle size distribution of the hydrometeors. The objective of these measurements and correlations was to obtain, by regression analyses, the M vs Z relationships that best described the situations at the different altitudes within the storm. These M vs Z relationships were then employed to convert the radar-measured Z_R values for the vehicle trajectories into corresponding values of liquid water content for the trajectories, which was the end information desired.

To determine the liquid water content of ice hydrometeors (snow and ice crystals) from aircraft spectral size data, such as obtained from the PMS instruments, three assumptive steps are required. First, it is necessary to assume something about the three-dimensional shape of the hydrometeors (or hydrometeor types) that are being sampled. Second, it is necessary to estimate their probable orientation during passage through, or impact on, the system aircraft instruments. These assumptions provide relationships between the "length measures" that define the geometry of the particles and those that are provided by the instruments. The basic objective is to estimate the volume of the particle(s) as accurately as possible from the aircraft measurements. Third, it is necessary to estimate the effective density of the ice-air mixture of the hydrometeors within these volumes, such that their equivalent water mass and equivalent melted diameters can be determined. These three assumptions, made for the full size range of the hydrometeors of the populations, permit the estimation of the liquid water content of the populations.

Subsequently, we will refer to these assumptive procedures as the process of L (physical size) to D (equivalent melted diameter) conversion.

Detailed investigations of aircraft spectral data (foil replicator data and PMS data) conducted at AFGL have shown that the M values for ice hydrometeors can vary widely depending on the particular assumptions of L to D conversion. Typically, even with observational knowledge of hydrometeor type, they can vary by as much as a factor of 5.

These investigations also led to the discovery of a

¹ Plank, V. G., 1974: A summary of the radar equations and measurement techniques used in the SAMS Rain Erosion Program at Wallops Island, Virginia. Special Rep. No. 172, AFCRL/SAMS Rep. No. 1, AFCRL-TR-74-0053, 108 pp. [NTIS AD 778 095].

² Barnes, A. A., J. I. Metcalf and L. D. Nelson, 1974: Aircraft and radar weather data analysis for PVM-5. Air Force Surveys in Geophysics, No. 297, AFCRL/Minuteman Rep. No. 1., AFCRL-74-0627, 47 pp. [NTIS AD B 004290].

spectral parameter that is much less subject to the effects of L to D conversion than is the spectral liquid water content M . We will describe this parameter in the following sections and illustrate the accuracy enhancement resulting from its use.

2. Derivations

For classified spectral data for ice hydrometeors, the liquid water content of any single sample is given by

$$M = C \sum_{i=1}^{i=n} N_i D_i^3 \text{ [g m}^{-3}\text{]}, \tag{1}$$

where N_i is the number concentration of the snow or ice particles in the successive diameter classes, where D_i is the mid-diameter (equivalent melted diameter) of the classes and

$$C = \frac{\pi}{6} \times 10^{-3} \rho, \tag{2}$$

where ρ is the density of liquid water, equal to 1.0 g cm^{-3} .

The radar reflectivity factor for these hydrometeors is given by

$$Z = \sum_{i=1}^{i=n} N_i D_i^6 \text{ [mm}^6 \text{ m}^{-3}\text{]} \tag{3}$$

and the number total of the particles; of all sizes within the population, is specified by

$$N_T = \sum_{i=1}^{i=n} N_i. \tag{4}$$

If we define a parameter

$$\alpha_i = N_i / N_T \tag{5}$$

which is the ratio of the number concentration of the particles in any given class to the number total, Eqs. (1) and (3) may be rewritten as

$$M = CN_T \sum_{i=1}^{i=n} D_i^3 \alpha_i, \tag{6}$$

$$Z = N_T \sum_{i=1}^{i=n} D_i^6 \alpha_i. \tag{7}$$

It is convenient at this point to assume initially that the spectral data are linearly classified, such that the diameter widths of the classes are commonly the same across the entire diameter range of the data.

For linear classification, the mid-diameter of the i th class of the data sample is related to the mid-diameter of the n th or last class, which contains the particles of the largest size, by

$$D_i = \frac{(2i - 1)}{(2n - 1)} D_n. \tag{8}$$

This presumes that the lower boundary of the first class is $D = 0$. Eq. (8) may then be substituted into Eqs. (6) and (7) to obtain

$$M = \frac{N_T C D_n^3}{(2n - 1)^3} \sum_{i=1}^{i=n} (2i - 1)^3 \alpha_i, \tag{9}$$

$$Z = \frac{N_T D_n^6}{(2n - 1)^6} \sum_{i=1}^{i=n} (2i - 1)^6 \alpha_i. \tag{10}$$

If Eq. (10) is solved for D_n^3 and substituted into Eq. (9),

$$M = \kappa Z^{0.5}, \tag{11}$$

where

$$\kappa = CF \sqrt{N_T}, \tag{12}$$

$$F = \frac{\sum_{i=1}^{i=n} (2i - 1)^3 \alpha_i}{[\sum_{i=1}^{i=n} (2i - 1)^6 \alpha_i]^{0.5}}. \tag{13}$$

The parameter κ is the spectral parameter of primary interest herein, with F being the "form factor" of the distribution, which describes the manner in which the number concentration of the particles in the different diameter classes are apportioned relative to each other, over the diameter range of the sample, and relative to the total number concentration values for the sample.

Parameter κ is identical whether found by solving Eq. (11) for κ or through the use of Eq. (12). Variations occurring in κ can be associated with changes in M and Z using Eq. (11) or in changes in N_T and F using Eq. (12).

The above equations were derived assuming linear classification. This is not necessary to the essential proof of the equations. For example, if the data are geometrically classified, with the class widths increasing in geometric progression with diameter size, it may be shown that Eqs. (11) and (12) still pertain but that the form factor becomes

$$F = \frac{\sum_{i=1}^{i=n} (D_n / D_{i_l})^{6i/(2n-1)} \alpha_i}{[\sum_{i=1}^{i=n} (D_n / D_{i_l})^{12i/(2n-1)} \alpha_i]^{0.5}}, \tag{14}$$

where D_{i_l} is the diameter at the lower boundary of the first size class and D_n the geometric mean diameter of the last or n th class. Actually, we can consider any specified manner of classification and demonstrate the same, except that particular equations for the form factor will differ. The general equation of the form factor for any non-specified system of classification in which the lower boundary of the first size class is $D = 0$ is given by

$$F = \frac{\sum_{i=1}^{i=n} D_i^3 \alpha_i}{[\sum_{i=1}^{i=n} D_i^6 \alpha_i]^{0.5}} \quad (15)$$

The values of the form factor have been determined for various types of spectral distributions and methods of classification. The classification method affects the values only in secondary degree. The values are primarily dependent on the nature of the distribution, e.g., whether its form is exponential, bimodal, uniform, monodispersed, etc. Typically, in normally observed distributions, the values will range between 0.1 and 1.0. The values cannot exceed 1.0 (monodispersed) but they can, under particular circumstances, be smaller than 0.1.³ It should also be noted that the form factor is an ambiguous parameter, which is to say that identical *F* values, within the range cited, can be obtained from different spectral distributions.

If the hydrometeor spectra are truncated at the lower diameter end (first few classes having zero contents), the *F* values are increased toward unity relative to the non-truncated counterparts.

With this background discussion of the form factor, we now return to a consideration of the spectral parameter κ , which is defined by Eq. (12) [or by Eq. (11), solved for κ]. The effects of *L* to *D* conversion on this parameter are much smaller than they are on either *M* or *Z*. We will demonstrate this in two ways; first, theoretically, and second, with reference to actual aircraft and radar data obtained during a flight through a storm.

3. Theoretical example

One common equation of *L* to *D* conversion is the power function relationship

$$D = \gamma L^\phi, \quad (16)$$

as used by Auer and Veal (1970, 1972) and Heymsfield (1972), for example, in which γ and ϕ have different values dependent on the hydrometeor type, i.e., large-snow, ice-crystals, etc.

We can utilize Eq. (16) to write the equations for *M*, *Z* and κ , from (6), (7), (12) and (15), as

$$M = CN_T \gamma^3 \sum_{i=1}^{i=n} L_i^{3\phi} \alpha_i, \quad (17)$$

$$Z = N_T \gamma^6 \sum_{i=1}^{i=n} L_i^{6\phi} \alpha_i, \quad (18)$$

³ The *F* values can be smaller than 0.1 for bimodal distributions in which there is a wide diameter separation between the modal peaks. They can also be smaller if the number concentration of the particles in the first, or the first few, of the diameter classes is relatively very large, compared to the number concentration versus size trend (usually quasi-exponential) that prevails in the other size classes beyond the first few.

$$\kappa = \frac{C\sqrt{N_T} \sum_{i=1}^{i=n} L_i^{3\phi} \alpha_i}{[\sum_{i=1}^{i=n} L_i^{6\phi} \alpha_i]^{0.5}} \quad (19)$$

These equations may be differentiated with respect to γ and ϕ (N_T does not change with *L* to *D* conversion) to obtain, in finite difference form,

$$\Delta M = 3CN_T \gamma^2 (\Delta\gamma \sum_{i=1}^{i=n} L_i^{3\phi} \alpha_i + \gamma \Delta\phi \sum_{i=1}^{i=n} L_i^{3\phi} \alpha_i \ln L_i), \quad (20)$$

$$\Delta Z = 6N_T \gamma^5 (\Delta\gamma \sum_{i=1}^{i=n} L_i^{6\phi} \alpha_i + \gamma \Delta\phi \sum_{i=1}^{i=n} L_i^{6\phi} \alpha_i \ln L_i), \quad (21)$$

$$\Delta\kappa = \frac{3C\sqrt{N_T}}{(\sum_{i=1}^{i=n} L_i^{6\phi} \alpha_i)^{0.5}} \left[\sum_{i=1}^{i=n} L_i^{3\phi} \alpha_i \ln L_i - \frac{(\sum_{i=1}^{i=n} L_i^{3\phi} \alpha_i)(\sum_{i=1}^{i=n} L_i^{6\phi} \alpha_i \ln L_i)}{\sum_{i=1}^{i=n} L_i^{6\phi} \alpha_i} \right] \Delta\phi. \quad (22)$$

To determine the relative changes in ΔM , ΔZ and $\Delta\kappa$ that would arise from *L* to *D* conversion, the above equations were evaluated for three types of ice hydrometeors and three values of liquid water content. The hydrometeor types chosen were ones of common reference by AFGL,⁴ namely, large snow, for which the presumed *M* vs *Z* relationship of regression for a family of spectral samples is $M = 0.00495 Z^{0.538}$, small snow, with $M = 0.0145 Z^{0.538}$ and ice crystals, of bullet-rosette type, with $M = 0.38 Z^{0.529}$. These *M* vs *Z* relationships were employed in conjunction with Eqs. (11) and (16)–(22) to form equation sets that could be solved with the specification of the form of the spectral distribution function together with assumptions about the values of γ and ϕ , of Eq. (16), and of $\Delta\gamma$ and $\Delta\phi$, which involved presumptions about the uncertainties of our knowledge of the *L* to *D* conversion equation.

The ice hydrometeors were assumed to be exponentially distributed, in number concentration versus their physical, or *L* size. The values of γ and

⁴ Plank, V. G., 1974: Hydrometeor parameters determined from the radar data of the SAMS Rain Erosion Program. Environmental Research Papers. No. 477, AFCRL/SAMS Rep. No. 2, AFCRL-TR-74-0249, 86 pp. [NTIS AD 786 454].

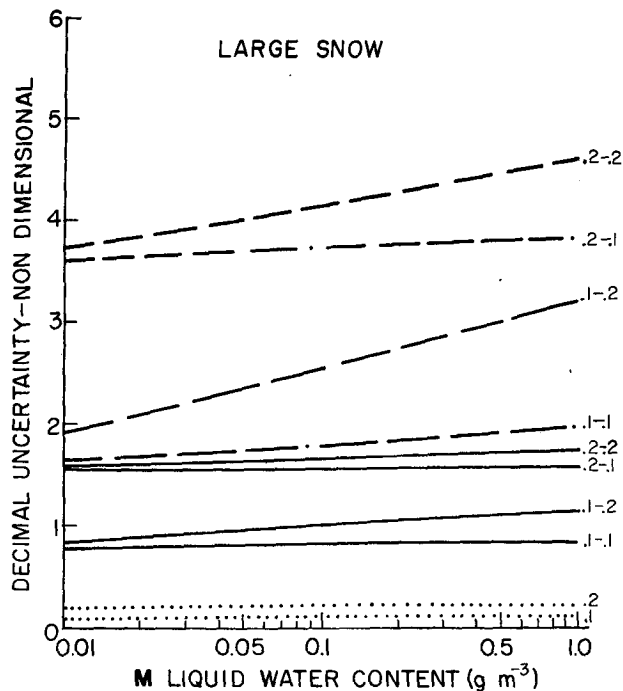


FIG. 1. Decimal uncertainties of radar reflectivity factor $\Delta Z/Z$ (dashed curves), liquid water content $\Delta M/M$ (solid curves) and spectral κ , $\Delta\kappa/\kappa$ (dotted curves) for large snow.

ϕ that were used were 0.4 and 0.875, for large snow, 0.324 and 0.805, for small snow, and 0.44 and 0.84, for ice crystals. These were AFGL values that were commonly associated with the types.⁵

The results of the investigations are illustrated in Figs. 1, 2 and 3. They are expressed in terms of decimal uncertainty, which is the ratio of the uncertainty to the nominal value of the quantity. Four uncertainty situations were considered for each of the ice hydrometeor types: (i) $\Delta\gamma = \Delta\phi = 0.1$ which in Figs. 1, 2 and 3 is symbolized by 0.1-0.1; (ii) $\Delta\gamma = 0.1$, $\Delta\phi = 0.2$, symbolized by 0.1-0.2; (iii) $\Delta\gamma = 0.2$, $\Delta\phi = 0.1$ or 0.2-0.1; and (iv) $\Delta\gamma = \Delta\phi = 0.2$, or 0.2-0.2. The 0.1 values are considered to be the typical, to be expected, values of uncertainty. The 0.2 values are assumed to be the probable maxima. The decimal uncertainties in M are indicated by the solid curves, those of Z by the dashed curves, and those of κ by the dotted curves. There are only two dotted curves per figure, as opposed to four for each of the others. This is because [see Eq. (22)] $\Delta\kappa$ changes only with $\Delta\phi$, and is not functionally dependent on $\Delta\gamma$.

From these figures, it is seen that the decimal un-

certainties of Z range from about 1.4 to 5.2. The uncertainties of M range from about 0.7 to 2.0. However, the uncertainties of κ vary only from about 0.1 to 0.35 (10-35%). This demonstrates that the κ values change much less with the uncertainties of L to D conversion, than do M or Z .

4. Observational example

The minimizing of uncertainty effects by use of the κ parameter, as indicated theoretically above, is actually attained in practice. For example, the data for a combined radar-aircraft measurement pass is illustrated in Fig. 4. The pass was flown on 30 January 1976 between 2150 and 2155 GMT, through a storm located over Wallops Island, Virginia. The AFGL, MC-130E aircraft was flying through aggregate snow at an average pass altitude of 2.74 km. The average temperature at flight altitude was -9.1°C . The numbers and sizes of the hydrometeors encountered during the pass were measured and recorded by PMS optical array spectrometers (Knollenberg, 1970). The aircraft was being tracked by the so-called "Spandar" radar (S band) at Wallops station, which is a NASA radar operated by the Applied Physics Laboratory of Johns Hopkins University. The radar Z values of the snow hydrometeors along the aircraft flight track were obtained from the radar range gate "one short" of the particular gate containing the aircraft echo. These

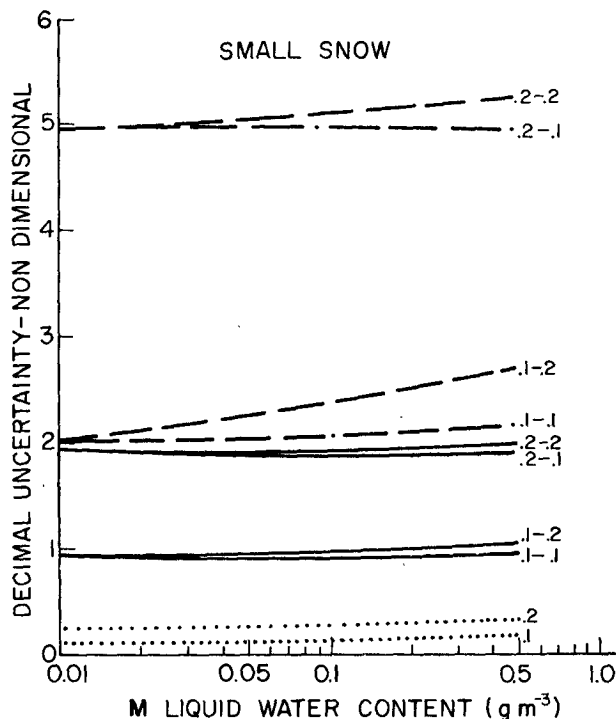


FIG. 2. As in Fig. 1 except for small snow.

⁵ Plank, V. G., 1977: Hydrometeor data and analytical-theoretical investigations pertaining to the SAMS Missile Flights of the 1972-73 season at Wallops Island, Virginia. Environmental Research Papers No. 603, AFGL/SAMS Rep. No. 5, AFGL-TR-77-0149, 239 pp. [NTIS AD A051 192].

Z_R values are shown by the heavy solid line of the upper diagram of Fig. 4.

If we presume, for the sake of illustration, that uncertainties existed regarding the type of snow being sampled during this pass, then, had it been assumed to be small snow, with the γ and ϕ values cited previously, which enter Eqs. (16), (17) and (18), the Z and M values for the PMS data of the pass would be as indicated by the identified curves of the two upper diagrams of Fig. 4. If, instead, the snow type had been presumed to be large snow, with the γ and ϕ values cited earlier, the Z and M curves would be changed to those also illustrated in the upper diagrams of Fig. 4. If, as an extreme assumption, the snow type had been presumed to be "wet snow,"⁶ the Z and M curves would be additionally changed as revealed in the diagrams.

The κ values for these three assumptions of snow type are shown in the bottom diagram of Fig. 4. The three curves fall "on top of one other" such that they cannot be individually identified at the scale of the plots.

It is apparent that the variability of κ for this aircraft pass, with presumed uncertainty of snow type, is much smaller than that of either M or Z . Thus, κ is a more stable parameter under L to D conversion than is spectral M [computed from eqs. (1)

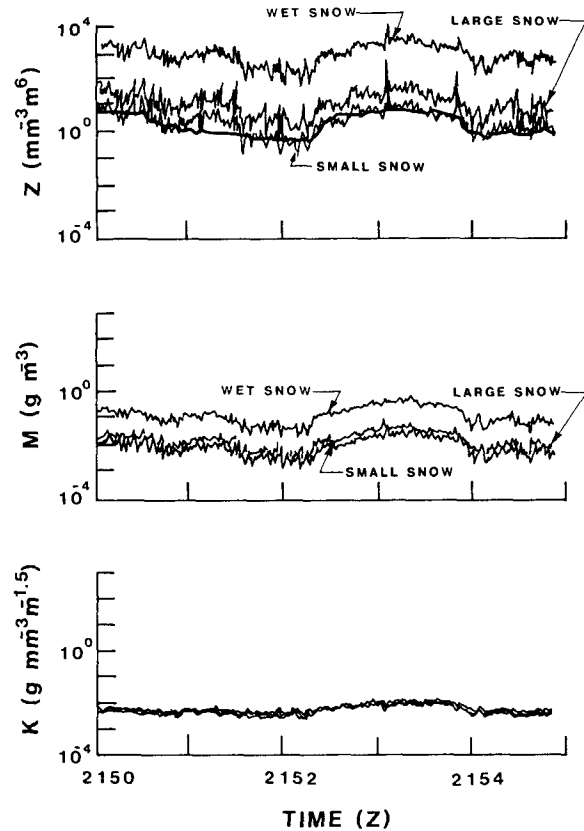


FIG. 4. Time plot of radar measured Z (heavy solid curve of upper diagram) and plots of aircraft spectral Z , M and κ corresponding to three different snow assumptions of L to D conversion (see text).

⁶ Cunningham, R. M., 1978: Analysis of particle spectral data from optical array (PMS) 1D and 2D sensors. AFGL-TR-78-0102, 6 pp. [NTIS AD A053 541].

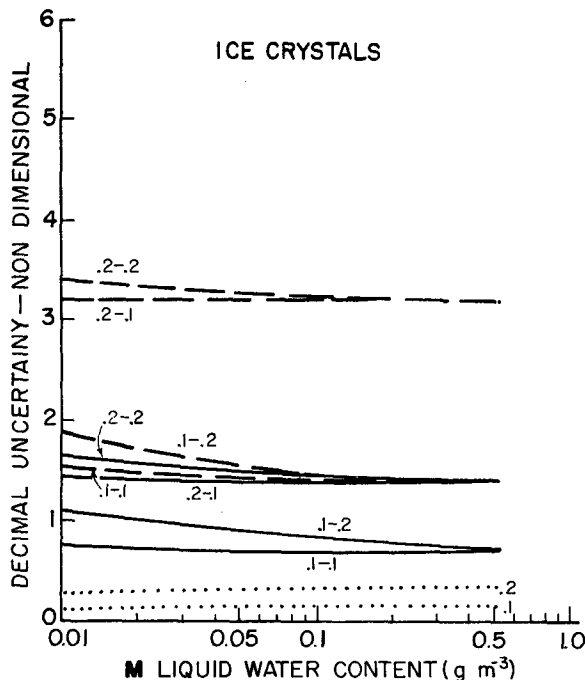


FIG. 3. As In Fig. 1 except for ice crystals.

and (2), with L to D assumption] or spectral Z [computed from eq. (3) with L to D assumption].

This stability of κ can be exploited to enhance the accuracy of regression analyses involving M and Z in situations of ice hydrometeors for which combined aircraft and radar data have been acquired. Such enhancement can be demonstrated with reference to the same aircraft-radar data that was employed in Fig. 4.

The left-hand diagrams of Fig. 5 show the scatter plots and log-log regression lines for the spectral M values (or aircraft M , M_A) plotted versus the radar measured values of Z , Z_R . The diagrams correspond to the three assumptions of L to D conversion discussed earlier. The regression equations are given above the diagrams and the log standard error values σ of data scatter about the regression lines, are indicated. The correlation coefficients r are also presented.

In contrast to this more or less conventional method of correlating aircraft M values and radar Z values, the middle diagrams of Fig. 5 show the values of derived M , M_D , computed from Eq. (11) written as

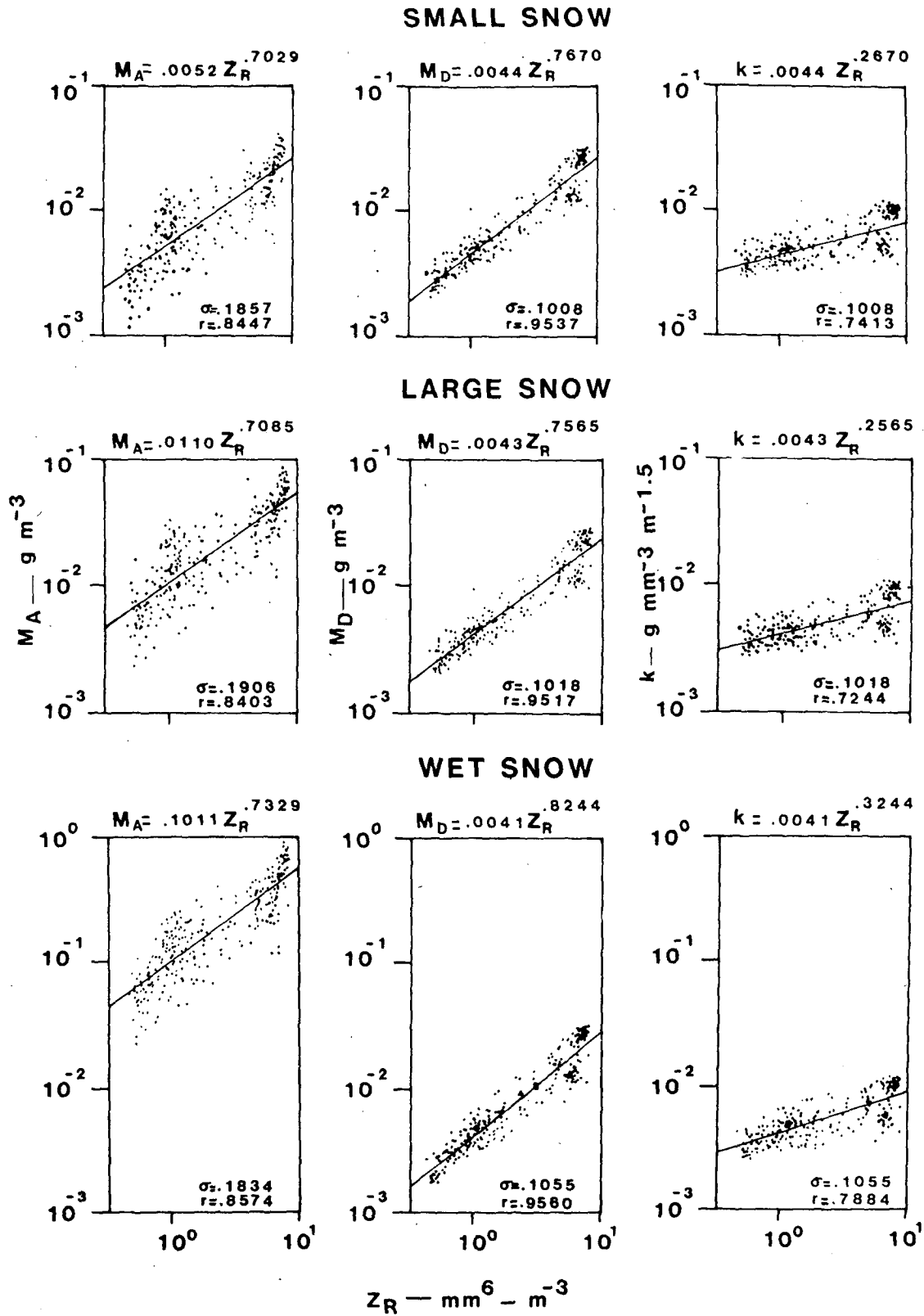


FIG. 5. Scatter diagrams and regression lines and equations for three assumptions of snow type. The left-hand diagrams show plots of aircraft M versus radar Z ; the middle diagrams show plots of "derived M " (text) versus radar Z ; the right-hand diagrams show plots of κ versus radar Z .

$$M_D = \kappa Z_R^{0.5}, \quad (23)$$

which are cross plotted versus the values of radar Z_R . Again, the regression equations and the σ and r values are noted.

The improvement of correlation resulting from the second method is apparent. The σ values are reduced; the correlation coefficients are enhanced and the regression equations reveal close agreement with one another irrespective of snow type assumption.

It is also of interest to illustrate the scatter plots and regressions of κ vs Z_R . These are shown in the right-hand diagrams of Fig. 5. It is seen that κ does not vary markedly with Z_R . In our experience at AFGL, we have found that κ sometimes increases with Z_R , as illustrated, that it sometimes is a constant and that it sometimes decreases with Z_R . The physical situations responsible for these differences have not yet been ascertained.

It should additionally be noted that the regression equations of κ vs Z_R and M_D vs Z_R are interrelated. Thus, if

$$\kappa = aZ_R^b, \quad (24)$$

then

$$M_D = aZ_R^{b+0.5}. \quad (25)$$

5. Summary

Uncertainty analyses and operational experience at AFGL have shown that, as demonstrated herein, the spectral parameter κ computed from aircraft size distribution data for ice hydrometeors is a much more stable parameter, under L to D conversion assumption, than is either spectral M or spectral Z .

This property of κ permits accuracy enhancement of regression analyses involving M and Z . For example, in our AFGL work, in which the problem is to assess the M values along vehicle trajectories for which the radar Z_R values are known (from scans made immediately after vehicle passage), we require accurate information about the M vs Z relations that pertain to the hydrometeors of the particular storm at all heights within the storm. To acquire this information so-called correlation runs are made before and after vehicle passage. In these runs, or passes, the aircraft is flown at a number of different altitudes within the storm and simultaneous aircraft PMS data and radar Z_R data are obtained

along the flight tracks. In later analyses, the κ values are computed from the PMS data and are correlated with the independently acquired radar Z_R values. Thus, the most accurate aircraft spectral parameter κ is being correlated against the most accurate measure of Z (radar Z_R being demonstratively more accurate than aircraft spectral Z)⁷ to obtain regression equations of the Eq. (24) form which are then immediately convertible into the Eq. (25) form.

It should be reemphasized that the κ concept of accuracy enhancement pertains strictly to ice hydrometeors and that it presumes that aircraft or other spectral data are being correlated with *independently* acquired Z_R values. There is no accuracy enhancement if spectral κ should be correlated against spectral Z since these are *dependent* quantities.

Spectral κ does have value by itself, however, in serving as a reference parameter to differentiate spectral differences between one sampling situation and another, as between the cloud or storm situations of one day and those of the next: This is true even for water hydrometeors (rain). Profiles of κ , together with those of N_T and F [see Eq. (12)], are also extremely useful in depicting the spectral properties of clouds and storms and suggesting the possible physical reasons for variation and difference. In this regard, it might be noted that our experience at AFGL has shown that κ is primarily dependent on the number total of hydrometeors (within the truncation size limits of the given instrument) and is generally only secondarily dependent on the form factor of the distribution (most observed distributions being quasi exponential).

REFERENCES

- Auer, A., and Veal, D., 1970: The dimensions of ice crystals in natural clouds. *J. Atmos. Sci.*, **27**, 919–926.
 Heymsfield, A. J., and Knollenberg, R. G., 1972: Properties of cirrus generating cells. *J. Atmos. Sci.*, **29**, 1358–1366.
 Knollenberg, R. G., 1970: The optical array: An alternative to extinction and scattering for particle size measurements. *J. Appl. Meteor.*, **9**, 86–103.

⁷ Crane, R. K., 1978: Evaluation of uncertainties in the estimation of hydrometeor mass concentrations using Spangar data and aircraft measurements. Sci. Rep. No. 1, Contract F19628-76-C-0069, Environmental Research and Technology, Inc., also AFGL-TR-78-0118, 107 pp. [NTIS AD A059 223].